

# Modeling of Mirror Surface Damage Effects on Beam Performance In a Laser-Driven IFE Power Plant

T.K. Mau, M.S. Tillack and M.R. Zaghloul

*Center for Energy Research, University of California-San Diego, La Jolla, CA 92093-0417, USA*

**Abstract**—Grazing incidence metal mirrors in laser-driven IFE power plants are subject to a variety of threats that result in damages leading to increased laser absorption, beam quality degradation and reduced laser-induced damage threshold. In this paper, we analyze the mirror reflectivity changes and wavefront distortions incident on the target using several modeling approaches, depending on the nature and size of the damage. We have developed a four-layer Fresnel solver to quantify the dependence of reflectivity on the thickness of surface contaminant and mirror protective coating, and their material properties, for a relevant range of incident angles. With a lossy contaminant like carbon, it is found that reflectivity decreases with thickness mainly due to surface dissipation, but this deleterious effect is diminished towards grazing incidence. For defect size small with respect to a wavelength, we have used Kerchhoff's wave scattering theory to evaluate degradation of the beam performance. For a damaged surface characterized by Gaussian statistics, we found that the average damage size needs to be less than one percent of the wavelength to avoid loss of beam intensity at 80° grazing incidence. Ray tracing techniques have been used to assess distortion in beam illumination profiles when the surface defect size is large compared to the incident wavelength. Simple bulk deformations of the mirror surface, typical of swelling due to thermal and gravity loads, have been studied.

## I. INTRODUCTION

The grazing incidence metal mirror (GIMM) [1] has been proposed as the final element of an optical system that provides optimum illumination of the DT fusion targets by the driver laser beams in order to achieve a full target implosion. Exposure to a variety of threats, including prompt neutron and gamma fluxes, x-ray and ionic emissions, and contamination from condensable target and chamber materials, could cause damage to the mirror resulting in increased laser absorption, beam quality degradation and reduced laser-induced damage threshold. This paper is aimed at addressing and quantifying the effects of these damages on the mirror performance, such as reflectivity and target illumination profile, using various wave modeling approaches.

For this study, a final optics arrangement based on the Prometheus-L Reactor design [2] will be employed. In this design there are 60 beamlines all focusing on the target at the center of the chamber. Each laser beam is collimated and refocused at a 90° bend, and reflected off a flat GIMM at a grazing angle of 80° to the mirror normal before reaching the target. The focal length of the focusing mirror is 30 m. with the distance from the GIMM to the target being 20 m. The

beam source is a KrF laser with a wavelength of 248 nm, while other sources such as the diode-pumped solid state laser (DPSSL) [3] at 345.5 nm have also been considered. The GIMM lowers the effective laser power flux without much loss of reflectivity, thus prolonging the mirror lifetime, and helps reducing neutron irradiation of the rest of the components in the optical train. The mirror reflecting surface is typically composed of a thin coating of aluminum on a silicon carbide substrate that provides structural support.

In this paper, modeling results are presented on damage effects on mirror and beam performance using the Prometheus-L final optics design as a reference. It is noted that the modeling tools developed will also provide analysis of laser-target experimental results [4] at UCSD, and help define design windows for the GIMM in a laser-driven IFE power plant in the ARIES study.

## II. MIRROR DEFECTS AND ANALYSIS APPROACHES

Depending on the type of threat, the mirror can sustain damages (or defects) that are dimensional or compositional in nature, each of which can be analyzed using a suitable approach. Dimensional defects involve induced geometrical changes in the mirror surface, and can be classified into two types according to the size  $\lambda$  of the defects relative to the incident wavelength  $\lambda_0$ . Gross deformations ( $\lambda > \lambda_0$ ) can be the direct consequence of faulty fabrication, neutron- and thermal-induced swelling, and gravity loads. This type of damage can best be analyzed by the ray tracing technique. On the other hand, for surface morphology with  $\lambda < \lambda_0$ , that are caused by laser-induced damage or thermomechanical load, the best analysis approach is by applying Kirchhoff's theory of light scattering by rough surfaces [5].

Compositional defects of the mirror are the result of surface contamination and involve local modifications of the material composition of the surface that alter its optical properties. For gross surface contamination, caused by neutron-induced transmutations or bulk re-deposition of impurities on the surface, a Fresnel solver for a one-dimensional multiple-layer medium [6] appears quite adequate. In the case of localized contaminants on the surface, such as aerosol, dust or debris from the surrounding, the Mie theory of particle scattering of light appears to be an appropriate technique.

Analyses on mirror dimensional defects and on gross surface contamination have been carried out and their results are

described in the following sections. The scattering of beams by particle contaminants on the mirror surface will be a subject of future investigations.

### III. FRESNEL ANALYSIS OF SURFACE CONTAMINANTS

Typically a mirror surface is composed of a thin coating (~100 nm) of aluminum on a silicon carbide substrate that provides structural support. It is found that a protective coating of  $\text{Al}_2\text{O}_3$ , a few nm thick, is always present on the Al surface due to natural oxidation. In an operating IFE chamber, it is likely that a layer of contaminant material(s) will be deposited on the oxide coating as a result of re-deposition. The Al coating thickness is designed to reflect and absorb all optical radiation before it reaches the substrate. Therefore, the mirror surface can be adequately described by a four-layer model (including the incident medium) as shown in Figure 1.

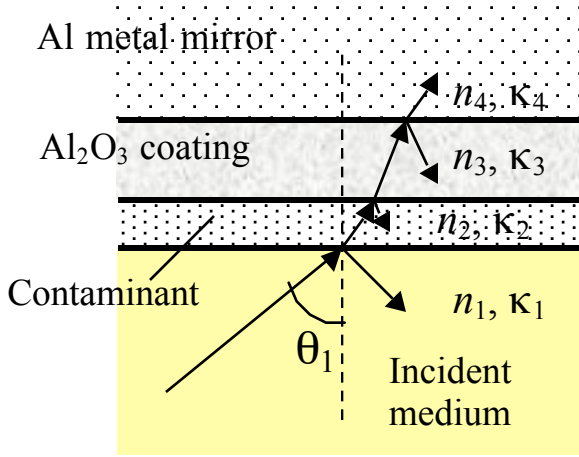


Fig.1. Four-layer model of mirror surface used in Fresnel analysis of contaminant effects on mirror and beam performance. Here,  $n_j$  and  $\kappa_j$  are the real and imaginary parts of the refractive index of medium  $j$ , and  $\theta_j$  is the beam incident angle.

In this model, each layer is assumed to be homogeneous, with uniform thickness  $d_j$ , and is characterized by a complex refractive index  $n_j = n_j + i\kappa_j$ , where  $n_j = (\epsilon_j \mu_j)^{1/2}$  and  $\kappa_j$  is the extinction coefficient for medium  $j$ . We will assume primarily TE or s-polarization for the beam. Refraction between adjacent layers is governed by Snell's law:

$$n_j \sin \theta_j = n_1 \sin \theta_1 \quad j = 2,3,4 \quad (1)$$

while reflectivity between two infinite media is given by Fresnel's relation:

$$r_{j,j+1} = \frac{n_j \cos \theta_j - n_{j+1} \cos \theta_{j+1}}{n_j \cos \theta_j + n_{j+1} \cos \theta_{j+1}} \quad (2)$$

The reflectivity from medium  $j$  is then given by [6]:

$$r_j = \frac{r_{j,j+1} + r_{j+1} e^{i2\theta_j}}{1 + r_{j,j+1} r_{j+1} e^{i2\theta_j}} \quad (3)$$

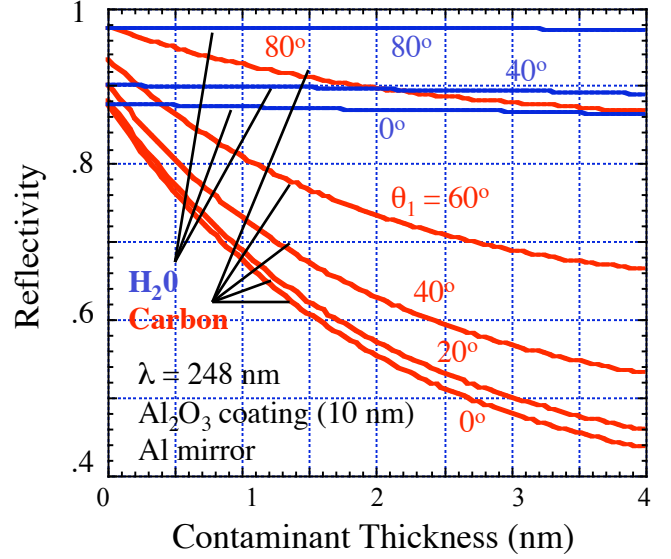


Fig. 2. Beam intensity reflectivity at the mirror surface for various carbon contaminant thickness at a number of incidence angles. Reflectivity for water is shown for comparison.

where  $\kappa_j = (2\epsilon_j \mu_j)^{1/2} n_j \cos \theta_j$ ,  $j = 2,3$ . The beam intensity reflectivity from the mirror can be obtained using  $R = |r_2|^2$ .

A large number of materials may be deposited on the mirror surface during power plant operation. To simplify our study, we use carbon as a representative contaminant material for a dry-wall chamber, using water as a reference material for comparison. The reflectivity is calculated using Eqs. (1)-(3) for various combinations of incidence angle  $\theta_1$ , contaminant thickness  $d_2$  and  $\text{Al}_2\text{O}_3$  coating thickness  $d_3$  at the KrF wavelength of 248 nm. In Fig. 2  $R$  is shown as a function of  $d_2$  for incidence angles ranging from  $0^\circ$  to  $80^\circ$ , at an  $\text{Al}_2\text{O}_3$  coating thickness of 10 nm. The first observation is that carbon degrades reflectivity very quickly as its thickness builds up. In comparison, there is little effect with water build-up since water at this wavelength is loss free while for carbon,  $\kappa \sim n$ . The deleterious effect on mirror reflectivity is strongly reduced as  $\theta_1$  approaches grazing incidence,  $\theta_1 = 80^\circ$ . It is also noted that in the absence of contaminant, reflectivity increases as grazing incidence is approached, when it reaches a value of 0.98 at  $\theta_1 = 80^\circ$ . From this figure, it is also clear that mirror reflectivity will not be able to tolerate a build-up of more than 1 nm of carbon even at grazing incidence. This requirement will relax for less lossy material such as water.

In Fig. 3, mirror reflectivity as a function of  $\text{Al}_2\text{O}_3$  coating thickness  $d_3$  is plotted for normal ( $0^\circ$ ) and grazing incidence ( $80^\circ$ ), and for cases with and without contaminant. As  $d_3$  is increased,  $R$  will pass through maximum and minimum values with a periodicity of a half-wavelength, indicative of interference effects within the loss-free dielectric medium. To maintain high reflectivity, there is a stringent limit on surface oxidation of Al, and the oxide thickness should not be allowed to exceed 10 nm for the case of grazing incidence.

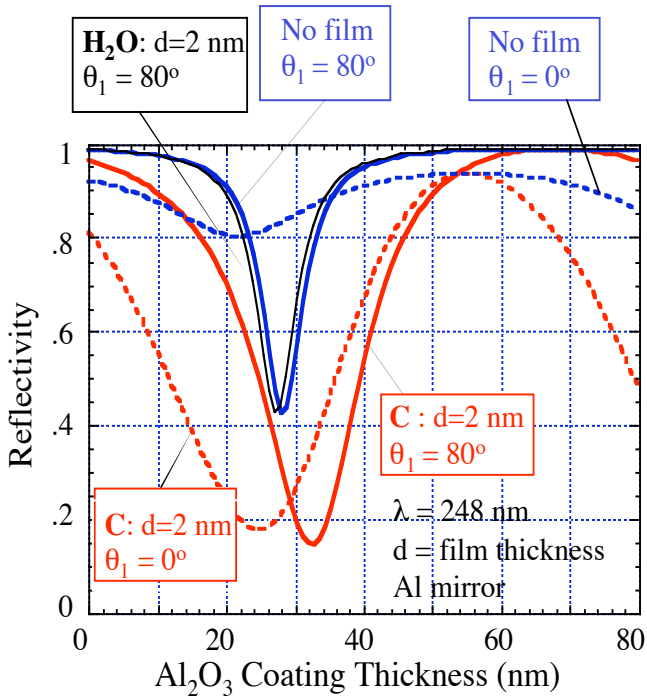
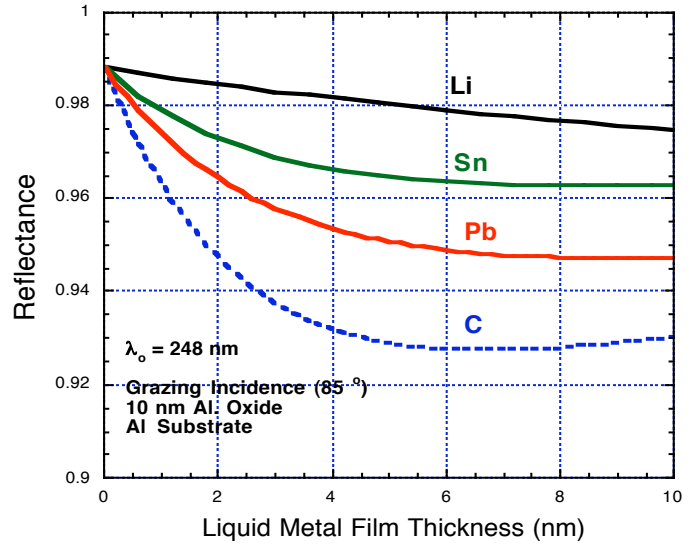


Fig. 3. Variation of mirror reflectivity with Al<sub>2</sub>O<sub>3</sub> coating thickness for normal and grazing incidence, and with and without carbon contaminant. The case of water is shown for comparison.

In a wetted-wall IFE chamber, it is possible that the GIMM be contaminated with a thin layer of liquid metal during plant operation. The significant conductivity present in these metals would lead to dissipation of the incident beam, and it is important to quantify their effect on the mirror reflective properties. A number of liquid metals have been studied, including Li, Sn and Pb, and the results are summarized in Fig. 4 for grazing incidence (85°) and  $\lambda = 248$  nm. Again one observes the degradation of  $R$  with increasing metal film thickness. Similar behavior of  $R$  is also obtained at  $\lambda = 354.5$  nm, with the deleterious effect less severe at the longer wavelength. From these studies, it is determined that the contamination level should be limited to less than 1 nm in order to meet the 1% obscuration requirement. Of the metals investigated, lead, which has optical properties similar to carbon in these wavelengths, is the most deleterious to mirror reflectivity. On the other hand, alkali metals such as Li, Na, with  $n \ll 1$  and  $\lambda \sim 1$ , are relatively benign.

#### IV. KIRCHHOFF THEORY OF LIGHT SCATTERING FROM ROUGH SURFACES

Mirror surface roughness as a result of laser-induced or thermo-mechanical damage simultaneously gives rise to wave scattering of two types: coherent in the specular direction and diffuse in other directions. The condition for coherent scattering to be dominant is determined by the so-called Raleigh parameter:  $R_a = 2\sigma \cos \theta_i / \lambda < \lambda/4$ , where  $\sigma$  is the rms height of the surface roughness and  $\theta_i$  is the incident angle. It is clear that the roughness of a surface depends on



the

Fig. 4. Variation of mirror reflectance as a function of liquid metal film thickness for a number of materials: Li, Sn, Pb, C. Carbon is included here for comparison.

properties ( $\epsilon, \mu$ ) of the wave being scattered. This type of wave behavior can be studied by invoking Kirshhoff's theory of wave scattering from random rough surfaces [5]. In this formulation, the scattered field is written in integral form as:

$$\mathbf{E}^{sc}(\vec{r}) = \int_{S_o} \mathbf{E}(\vec{r}_o) \frac{\partial G(\vec{r}, \vec{r}_o)}{\partial n_o} - G(\vec{r}, \vec{r}_o) \frac{\partial \mathbf{E}(\vec{r}_o)}{\partial n_o} d\vec{S}_o$$

where  $S_o$  is the scatterer (mirror) surface,  $G$  is the full-space Green's function,  $\mathbf{E}$  is the sum of the incident and scattered field, and  $n_o$  is the surface normal. With simplifying approximations [5], the average scattered field can be recast as  $\langle \mathbf{E}^{sc} \rangle = \langle k_z \rangle \mathbf{E}_o^{sc}$  where  $\mathbf{E}_o^{sc}$  is the scattered field from a smooth surface,  $\langle k_z \rangle$  is the characteristic function of the rough surface, and  $k_z$  is a wavenumber normal to the mean surface.

For cumulative induced damages, one can assume Gaussian surface statistics which gives  $\langle k_z \rangle = \exp\{-k_z^2 \sigma^2/2\}$ . The resultant specularly reflected coherent intensity is then given by  $I_{coh} = I_o \exp\{-g\}$  where  $I_o$  is reflected intensity from smooth surface and  $g = 4R_a^2$ . The intensity degradation factor  $e^{-g}$ , is plotted as a function of normalized surface roughness,  $\sigma/\lambda$ , for three incidence angles, in Fig. 5. The reflected intensity decreases very rapidly with increasing surface roughness for all incidence angles. At grazing incidence, the reflected intensity is much less affected by surface roughness than at near normal incidence. Note that at  $\theta_i = 80^\circ$  and  $\sigma/\lambda = 0.1$ , the value of degradation  $\exp\{-g\}$  is 0.97. The general conclusion is that to void loss of beam intensity, the average surface roughness needs to be less than 1% of the wavelength.

## V. RAY TRACING ANALYSIS OF GROSS DEFORMATION EFFECT

For gross surface deformation such as swelling due to thermal or gravity load, or fabrication defect, the technique of ray tracing has been used to assess its effect on the beam spot size at the target location. The Prometheus-L final optics design [2] is used as an example for the investigation. Here the GIMM half-diameter  $a_m = 0.2$  m,  $\theta_i = 80^\circ$ , the target half-diameter is 3 mm, and the beam spot size  $a_{sp} = 0.64$  mm. Assume that the normally flat GIMM surface acquires a curvature  $r_c$  under thermal stress or due to fabrication defect. The surface defect is then defined as a surface sag:  $\Delta = a_m^2/2r_c$  which describes the resultant shape of the deformation. A series of ray tracing runs of the optical design software ZEMAX indicate that the beam spot size at the target enlarges and the cross section evolves from circular to elliptical as the surface sag increases. The consequence is overlapping of focal spots from adjacent beams thus modifying the target illumination profile. At the same time, the intensity profile for each beam spot becomes nonuniform. For a mirror of 0.3 m half-diameter, the limiting mirror surface sag for grazing incidence is approximately  $\Delta < 0.2 \mu\text{m}$ , if the non-uniformity in illumination is constrained to less than 1%. At this limit, the spot size is increased by about 10%.

## VI. SUMMARY AND DISCUSSIONS

A number of modeling approaches have been used to assess the effects of mirror surface damage on GIMM and driver beam performance in an IFE power plant. The chosen approach depends on the characteristics and size of the surface deformation compared to the wavelength. The scope of the analysis so far is based on a specific final optics system of the Prometheus-L IFE power plant design study, and certain simplifications have been introduced to obtain a meaningful assessment.

For compositional damage involving gross surface contamination, the Fresnel solver has been used and it is found that  $\sim 1$  nm contaminant thickness can be tolerated to limit the degradation of reflectivity to 1-2%. Kirchhoff theory of wave scattering from rough surfaces found that microscopic defects cannot exceed 1% of wavelength in size for Gaussian surface statistics. Finally preliminary ray tracing calculations indicate that gross surface swelling with surface sag of  $< 0.2 \mu\text{m}$  can be tolerated to limit non-uniformity in beam illumination to 1%.

It is also observed that grazing incidence mirrors not only permit longer mirror lifetime and improve reflectivity, they also appear to be more tolerant to induced surface damages in the form of contaminant build-up and accumulated surface roughness. Of the several liquid metals investigated as a possible contaminant in a wetted-wall power plant, lead is

most deleterious to mirror performance, while Na and Li are rather benign.

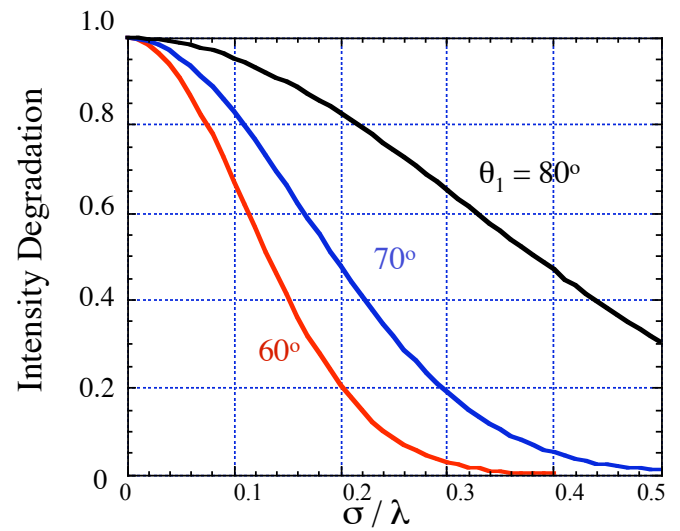


Fig. 5. Degradation of reflected beam intensity as a function of average surface roughness and incidence angle.

## ACKNOWLEDGEMENT

This work is supported by the US Department of Energy Grants N000173-01-1-G906 and DE-FC03-95ER54299.

## REFERENCES

- [1] R.L. Bieri and M.W. Gquinan, "Grazing Incidence Metal Mirrors as the Final Element in a Laser Driver for Inertial Confinement Fusion," *Fusion Technology*, Vol. 19, pp. 673-678, May 1991.
- [2] "Inertial Fusion Energy Reactor Design Studies: Prometheus Final Report", Report DOE/ER-54101, March 1992.
- [3] C. D. Orth, S. A. Payne, and W. F. Krupke, "A Diode Pumped Solid State Laser Driver for Inertial Fusion Energy," *Nuclear Fusion*, Vol. 36, pp. 75-116, 1996.
- [4] M.R. Zaghoul, M.S. Tillack, and T.K. Mau, "Sensitivity of Metal Mirrors to Laser-Induced Damage Under Long-Term Exposure at Shallow Angle of Incidence," this *Symposium*.
- [5] J.A. Ogilvy, "Theory of Wave Scattering from Random Rough Surfaces," Adam Hilger, IOP Publishing, 1991.
- [6] M. Born and E. Wolf, "Principles of Optics," 7th Edition, Cambridge University Press, 1999.